Synergistic Ru-Mediated Activation of CoP/Co Heterostructures on Carbon Nanofibers toward Efficient Hydrogen Evolution

Xiaoyang Wei[ab], Zhangsen Chen[bc], Xinpeng Ma[a], Shuhui Sun[b,], Chun-Gang Yuan[a,*]*

[a] *Hebei Key Laboratory of New Energy Environmental Safety and Resource Utilization, Department of Environmental Science & Engineering, North China Electric Power University, Baoding 071000, China.*

[b] *Institute National de la Recherche Scientifique (INRS), Center Énergie Matériaux Télécommunications, Varennes, Québec, J3X 1P7, Canada*

[c] *Department of Chemical Engineering, McGill University, Montreal, Quebec, H3A 0C5, Canada*

[*] *Corresponding emails: cgyuan@ncepu.edu.cn (C. Y.); shuhui.sun@inrs.ca (S. S.)*

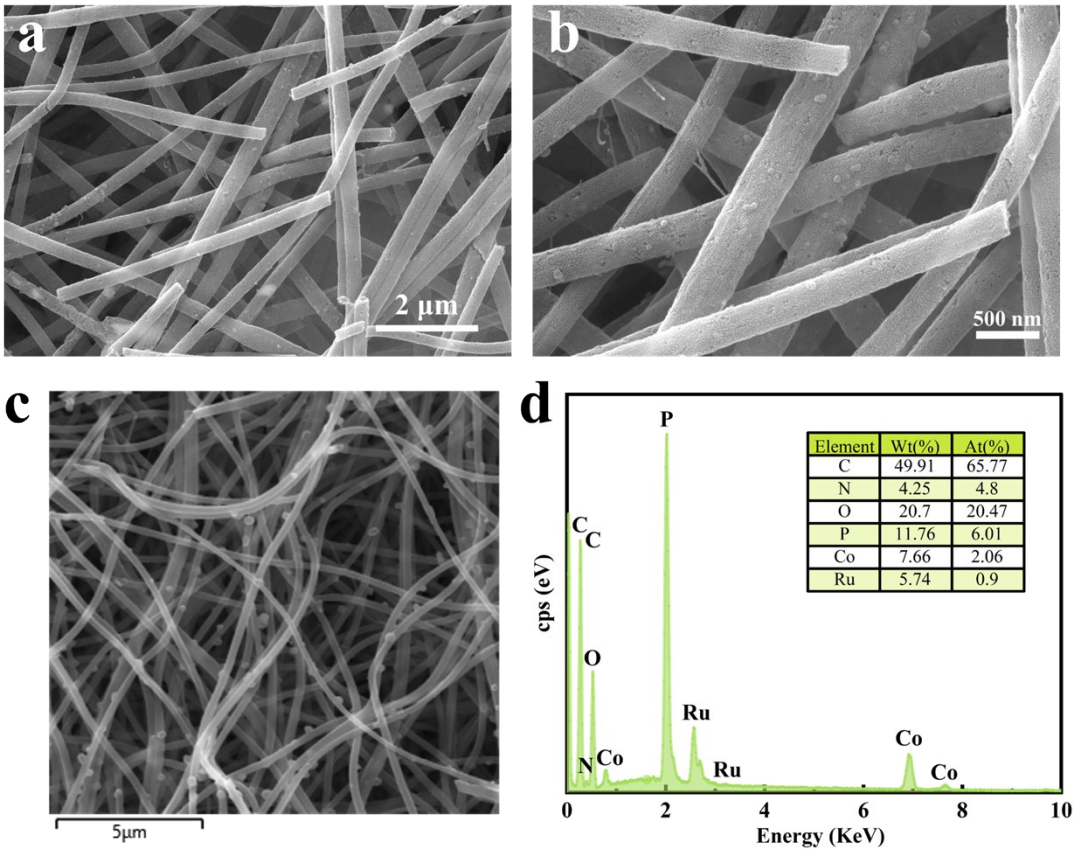

Fig. S1. (a-b) EM images of Co-NCNFs. (c) SEM image and (d) EDS of Ru-CoP/Co-NCNFs.

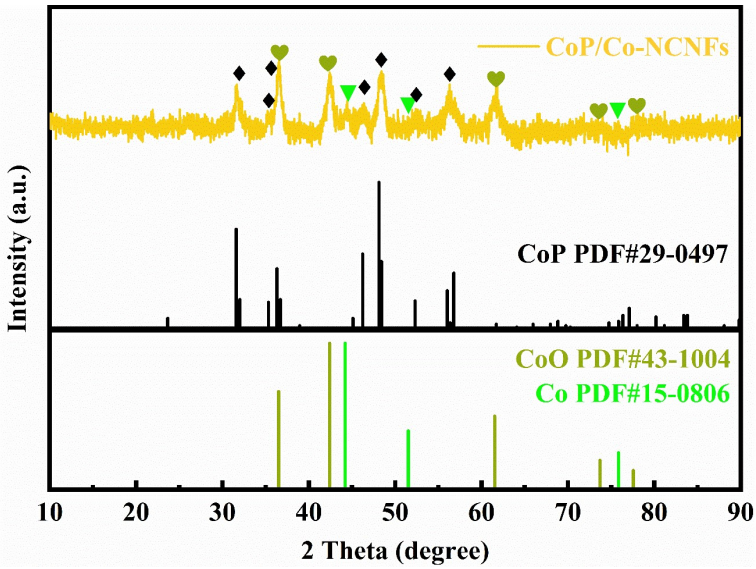

Fig. S2. XRD patterns of CoP/Co-NCNFs.

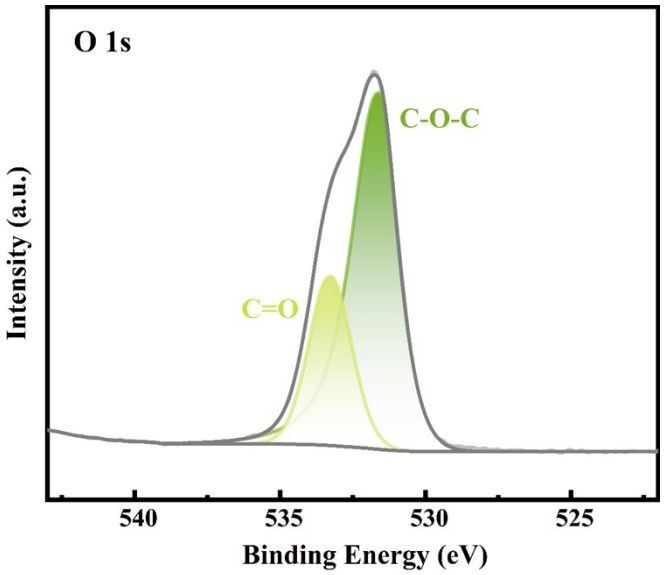

Fig. S3. XPS high-resolution O 1s spectra of the Ru-CoP/Co-NCNFs.

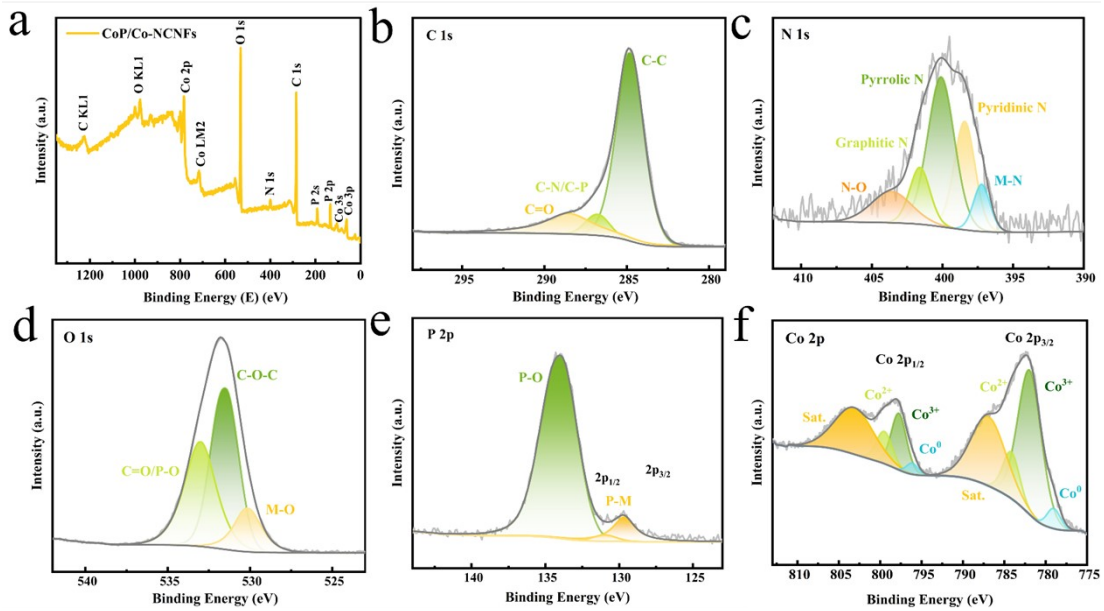

Fig. S4. (a) XPS survey spectrum and high-resolution (b) C 1s, (c) N 1s, (d) O 1s, (e) P 2p, and (f) Co 2p spectra of the CoP/Co-NCNFs.

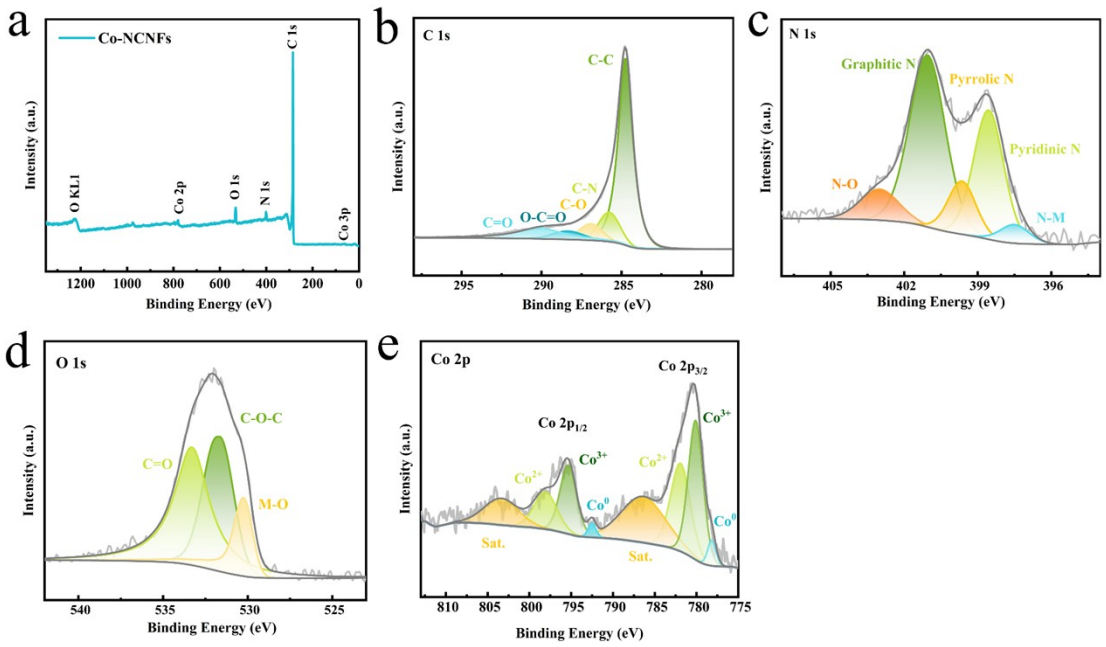

Fig. S5. (a) XPS survey spectrum and high-resolution (b) C 1s, (c) N 1s, (d) O 1s, and (e) Co 2p spectra of the Co-NCNFs.

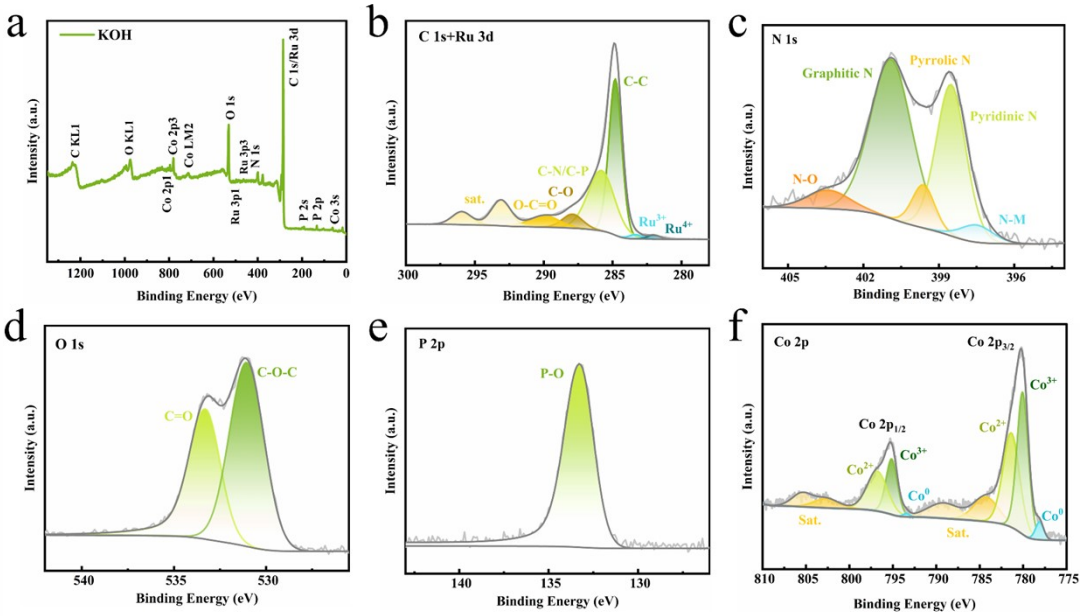

Fig. S6. (a) XPS survey spectrum and high-resolution (b) C 1s+Ru 3d, (c) N 1s, (d) O 1s, (e) P 2p, and (f) Co 2p spectra of the Ru-CoP/Co-NCNFs after chronoamperometric testing in 1.0 M KOH solution.

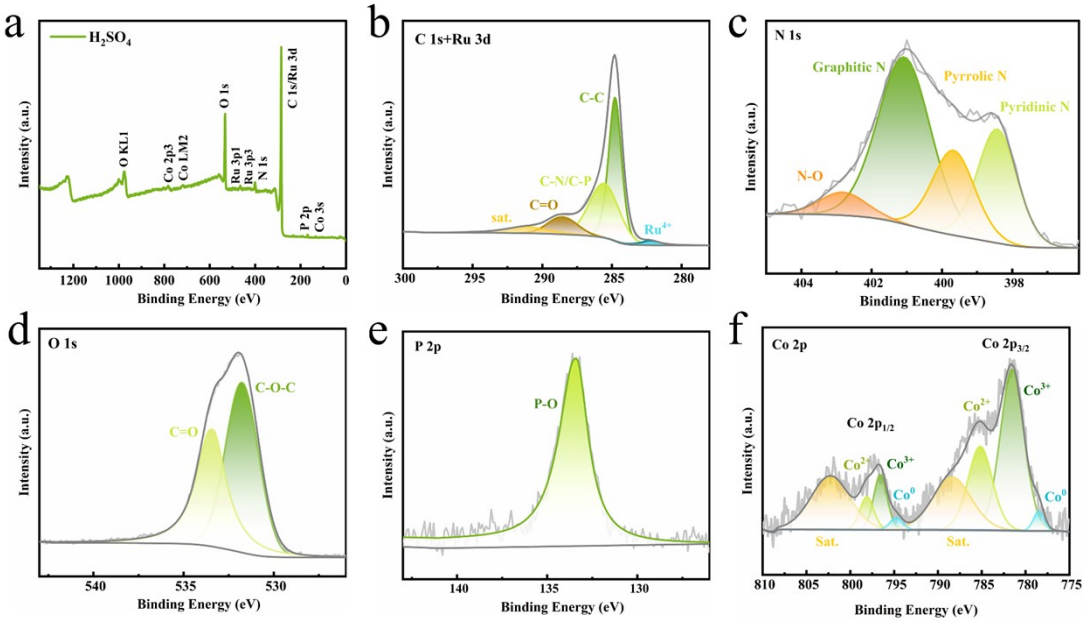

Fig. S7. (a) XPS survey spectrum and high-resolution (b) C 1s+Ru 3d, (c) N 1s, (d) O 1s, (e) P 2p, and (f) Co 2p spectra of the Ru-CoP/Co-NCNFs after chronoamperometric testing in 0.5 M H_2SO_4 solution.

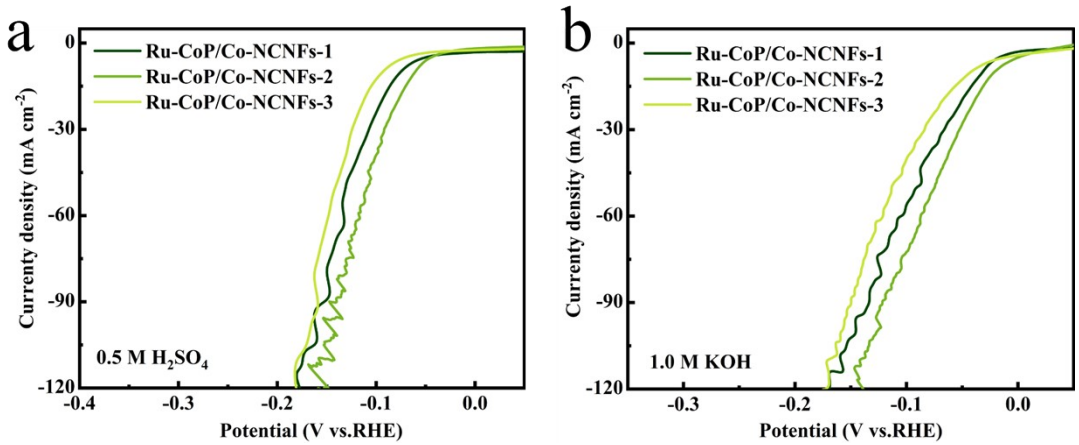

Fig. S8. Polarization curves for the different contents of Ru (a) in 0.5 M H_2SO_4 and (b) 1.0 M KOH solution.

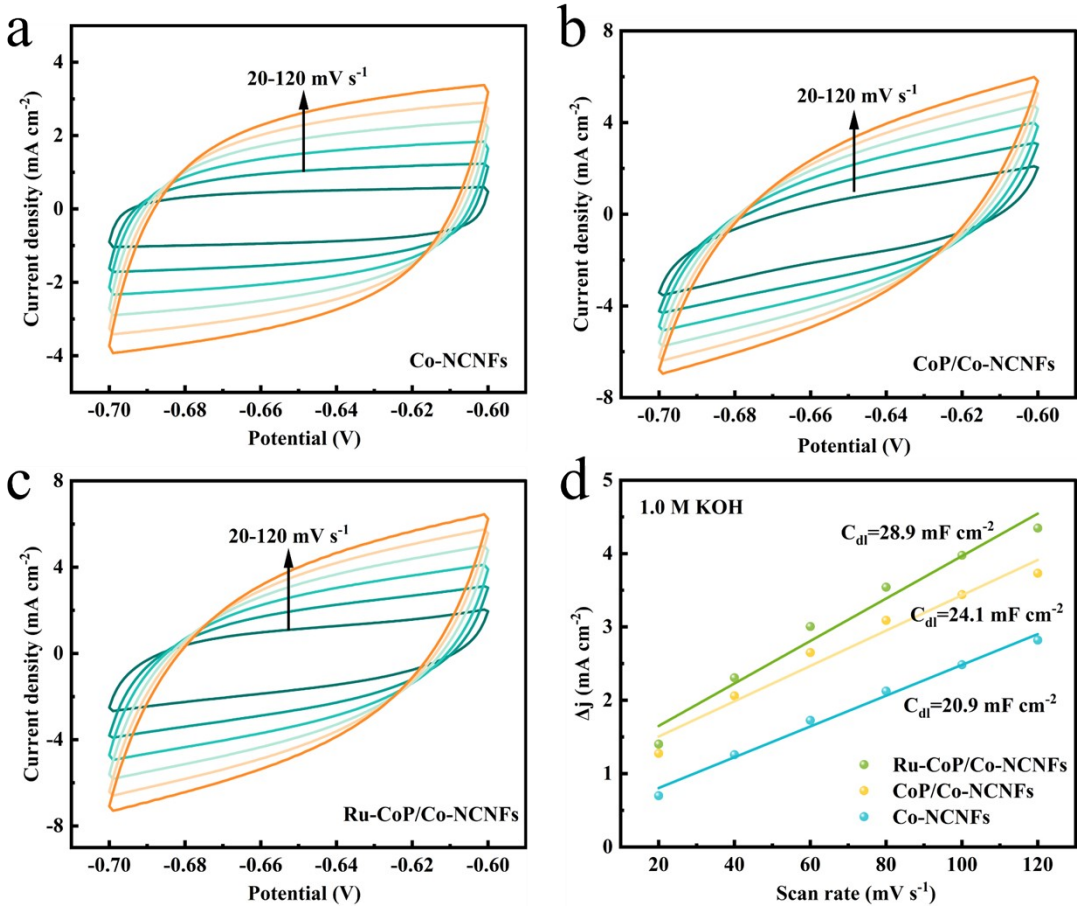

Fig. S9. (a-c) CV curves with 20 to 120 mV s^{-1} scan rate and (d) C_{dl} for different samples in 1.0 M KOH solution.

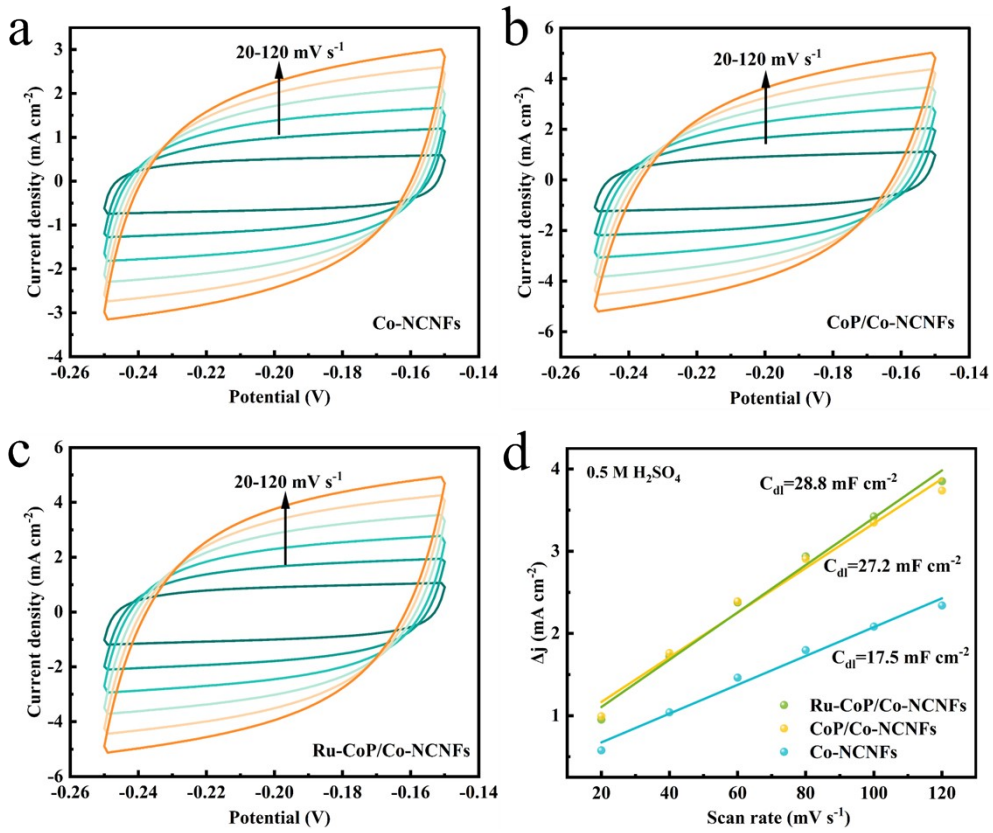

Fig. S10. (a-c) CV curves with 20 to 120 mV s^{-1} scan rate and (d) C_{dl} for different samples in 0.5 M H_2SO_4 solution.

The turnover frequency (TOF) for HER was calculated by the following equation：

$$TOF = \frac{I}{Q} = \frac{|j|S}{2nF}$$

Where I (A) is the current, Q (C) is voltammetric charges, $|j|$ ($A \cdot cm^{-2}$) is the current density, S is the geometric area of the working electrode (1.0 cm^2), F is the Faraday constant (96485 $C \cdot mol^{-1}$), and n is the number of active sites (mol). 2 is the electron transfer numbers of HER. The number of active sites (n) was calculated by the method previously reported. CV was used to scan a voltage range of 0-0.4V (vs. RHE) at a rate of 50 mV s^{-1} in a 1.0 M PBS solution.

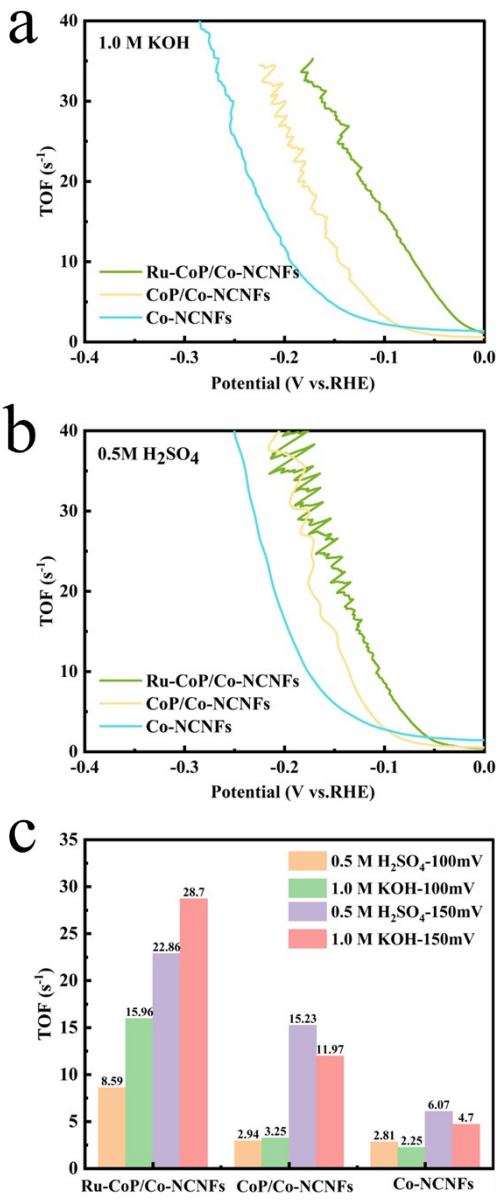

Fig. S11. TOF curves of the different samples in (a) 1.0 M KOH, (b) 0.5 M H_2SO_4 solutions, and (c) comparison of values at different potentials.

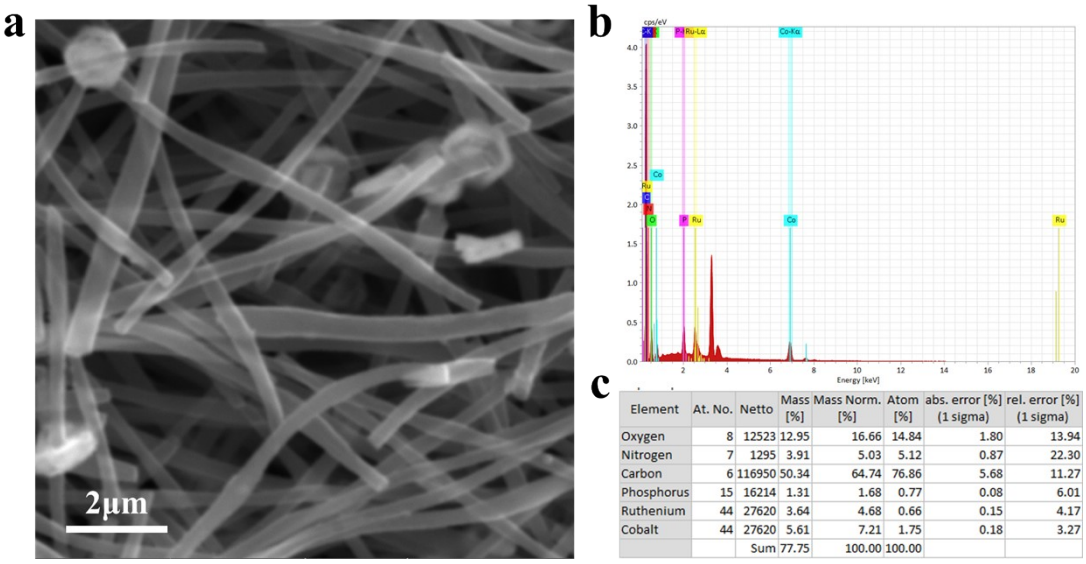

c

Element	At. No.	Netto	Mass [%]	Mass Norm. [%]	Atom [%]	abs. error [%] (1 sigma)	rel. error [%] (1 sigma)
Oxygen	8	12523	12.95	16.66	14.84	1.80	13.94
Nitrogen	7	1295	3.91	5.03	5.12	0.87	22.30
Carbon	6	116950	50.34	64.74	76.86	5.68	11.27
Phosphorus	15	16214	1.31	1.68	0.77	0.08	6.01
Ruthenium	44	27620	3.64	4.68	0.66	0.15	4.17
Cobalt	44	27620	5.61	7.21	1.75	0.18	3.27
		Sum	77.75	100.00	100.00		

Fig. S12. (a) SEM image, (b) EDS, and (c) element content table of Ru-CoP/Co-NCNFs after stability test in 1.0 M KOH.

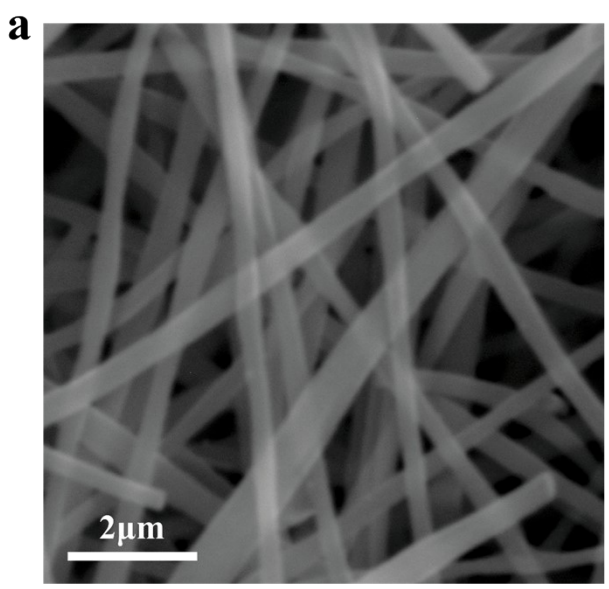

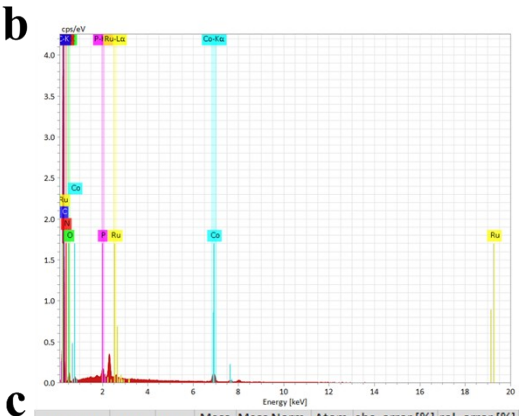

c

Element	At. No.	Netto	Mass [%]	Mass Norm. [%]	Atom [%]	abs. error [%] (1 sigma)	rel. error [%] (1 sigma)
Oxygen	8	1653	8.83	8.83	7.17	1.82	20.63
Nitrogen	7	363	5.82	5.82	5.41	1.85	31.78
Carbon	6	50902	79.51	79.51	86.05	9.45	11.88
Phosphorus	15	2226	0.81	0.81	0.34	0.07	8.54
Ruthenium	44	1544	0.88	0.88	0.11	0.08	8.96
Cobalt	27	3325	4.15	4.15	0.92	0.17	4.15
		Sum	**100.00**	**100.00**	**100.00**		

Fig. S13. (a) SEM image, (b) EDS, and (c) element content table of Ru-CoP/Co-NCNFs after stability test in 0.5 M H_2SO_4.

Table S1. Elemental content in different samples and after stability testing by XPS.

Catalysts	C (At %)	O (At %)	N (At %)	P (At %)	Co (At %)	Ru (At %)
Ru-CoP/Co-NCNFs	36.99	34.78	3.22	12.52	11.19	2.96
CoP/Co-NCNFs	43.28	25.53	2.11	6.09	25.99	-
Co-NCNFs	88.22	6.85	3.08	-	1.85	-
Ru-CoP/Co-NCNFs-H_2SO_4	71.82	17.47	4.08	1.32	3.54	1.79
Ru-CoP/Co-NCNFs-KOH	71.52	17.41	4.06	1.32	3.51	1.78

Table S2. The value of j_0 of the different samples in 0.5 M H_2SO_4 and 1.0 M KOH solutions.

Catalysts	j_0 (mA cm^{-2})	j_0 (mA cm^{-2})
	0.5 M H_2SO_4	1.0 M KOH
Ru-CoP/Co-NCNFs	6.52	2.48
CoP/Co-NCNFs	4.99	1.26
Co-NCNFs	0.96	0.53
RuCoP/CP	1.16	0.79
RuCoP/CC	1.14	0.70
20% Pt/C	6.80	4.46

Table S3. EIS parameters of the different samples in 0.5 M H_2SO_4 and 1.0 M KOH solutions.

Catalysts	R_s (Ω)	R_{ct} (Ω)	R_s (Ω)	R_{ct} (Ω)
	0.5 M H_2SO_4		1.0 M KOH	
Ru-CoP/Co-NCNFs	5.58	6.28	4.09	12.17
CoP/Co-NCNFs	5.76	6.70	5.56	17.51
Co-NCNFs	6.08	9.36	7.88	23.55

Table S4. C_{dl} and ECSA values of the different samples in 0.5 M H_2SO_4 and 1.0 M KOH solutions.

Catalysts	C_{dl} (mF cm^{-2})	ECSA (cm^{-2} mg^{-1})	C_{dl} (mF cm^{-2})	ECSA (cm^{-2} mg^{-1})
	0.5 M H_2SO_4		1.0 M KOH	
Ru-CoP/Co-NCNFs	28.8	720.0	28.9	722.5
CoP/Co-NCNFs	27.2	680.0	24.1	602.5
Co-NCNFs	17.5	437.5	20.9	522.5

Table S5. Comparison of the catalytic performance of reported HER catalysts in 1.0 M KOH solution.

Catalysts	η_{10} (mV)	Tafel (mV dec^{-1})	Stability	Ref.
Ru-CoP/Co-NCNFs	21	59.5	retaining 90% after 200 h 10,000 cycles	This work
Ru-CoP_x/NF	41	68	12h	[1]
Ru-CoP/CC	44	64	60 h	[2]
Ru@CoP/CC	48	103	27.8h	[3]
CoP@NC-Ru	35	72	5000 cycles	[4]
Ru/B-CoP	52	63.6	20 h	[5]
Ru-CoP-2.5 NAs	52	70.1	50 h	[6]
Ru-CoP/CC-2	45	98.11	20 h	[7]
Ru, Ni-CoP	45	53.9	40 h	[8]
Ru-CoP/CDs	51	73.4	2000 cycles	[9]
MnRuPOGO-500	27	57.35	48 h	[10]
Ru-MoS_2-Mo_2C/TiN	25	58	30 h	[11]

Table S6. Comparison of the catalytic performance of reported HER catalysts in 0.5 M H_2SO_4 solution.

Catalysts	η_{10} (mV)	Tafel (mV dec^{-1})	Stability	Ref.
Ru-CoP/Co-NCNFs	60	50.6	retaining 90% after 200h 6000 cycles	This work
Ru-CoPx/NF	73	59	12 h	[1]
Ru@CoP/CC	66	84	27.8h	[3]
Ru-CoP/NC	98	56	-	[12]
MnRuPOGO-500	109	38.55	60 h	[10]
CNT−V−Fe−Ru	64	51	20 h	[13]
RuMo/NCN	82	54	12 h	[14]
NiZn@C-CoP	89	74	24 h	[15]
Br-Ru-RuO_2/MCC	77	49	12 h	[16]
NF@CoFeP	82	60	50 h	[17]
$CoSe_2$/a-CoP	65	54	50 h	[18]

References

1 Shang, M.; Zhou, B.; Liu, D.; Yu, M.; Zhang, Y.; Xiao, W.; Yang, P.; Xu, G.; Wu, Z.; Wang, L. Modulated Co-P bond via ruthenium doping to facilitate spearhead-like CoP_x for overall water splitting. Int. J. Hydrog. Energy 2024, 49, 15-24.

2 Liu, S.; Li, Z.; Chang, Y.; Gyu, K.M.; Jang, H.; Cho, J.; Hou, L.; Liu, X. Substantial Impact of Built-in Electric Field and Electrode Potential on the Alkaline Hydrogen Evolution Reaction of Ru-CoP Urchin Arrays. Angew. Chem. Int. Ed. 2024, 63, e202400069.

3 Sun, D.; Qiang, P.; Yu, Y.; Zhang, J.; Huang, L.; Qu, Y.; Su, Q.; Xu, B. Electronic modulation with Ru nanoclusters decorated CoP nanowire arrays for alkaline and acidic hydrogen evolution reaction. Int. J. Hydrog. Energy 2024, 59, 1205-1213.

4 Kumar, M.M.; Aparna, C.; Nayak, A.K.; Waghmare, U.V.; Pradhan, D.; Raj, C.R. Surface Tailoring-Modulated Bifunctional Oxygen Electrocatalysis with CoP for Rechargeable Zn-Air Battery and Water Splitting. ACS Appl. Mater. Interfaces 2024, 16, 3542-3551.

5 Wang, Y.; Li, B.; Xiao, W.; Wang, X.; Fu, Y.; Li, Z.; Xu, G.; Lai, J.; Wu, Z.; Wang, L. Atomic doping modulates the electronic structure of porous cobalt phosphide nanosheets as efficient hydrogen generation electrocatalysts in wide pH range. Chem. Eng. J. 2023, 452, 139175.

6 Liu, Y.; Xu, S.; Zheng, X.; Lu, Y.; Li, D.; Jiang, D. Ru-doping modulated cobalt phosphide nanoarrays as efficient electrocatalyst for hydrogen evolution reaction. J. Colloid Interface Sci. 2022, 625, 457-465.

7 Cui, H.; Jiang, M.; Tan, G.; Xie, J.; Tan, P.; Pan, J. The In-situ Growth of Ru Modified CoP Nanoflakes on Carbon Clothes as Efficient Electrocatalysts for HER. ChemElectroChem 2022, 9, 287-288.

8 Song, Y.; Cheng, J.; Liu, J.; Ye, Q.; Gao, X.; Lu, J.; Cheng, Y. Modulating electronic structure of cobalt phosphide porous nanofiber by ruthenium and nickel dual doping for highly-efficiency overall water splitting at high current density. Appl. Catal. B: Environ. 2021, 298, 120488.

9 Song, H.; Wu, M.; Tang, Z.; Tse, J.S.; Yang, B.; Lu, S. Single Atom Ruthenium-Doped CoP/CDs Nanosheets via Splicing of Carbon-Dots for Robust Hydrogen Production. Angew. Chem. Int. Ed. 2021, 60, 7234-7244.

10 Ren, L.; Yang, D.; Yang, J. Ruthenium-manganese phosphide nanohybrid supported on graphene for efficient hydrogen evolution reaction in acid and alkaline conditions. Int. J. Hydrog. Energy 2022, 47, 13876-13886.

11 Hoa, V.H.; Tran, D.T.; Prabhakaran, S.; Kim, D.H.; Hameed, N.; Wang, H.; Kim, N.H.; Lee, J.H. Ruthenium single atoms implanted continuous MoS_2-Mo_2C heterostructure for high-performance and stable water splitting. Nano Energy 2021, 88, 106277.

12 Hao, Y.; Xue, H.; Sun, J.; Guo, N.; Song, T.; Sun, J.; Wang, Q. Tuning the Electronic Structure of CoP Embedded in N-Doped Porous Carbon Nanocubes Via Ru Doping for Efficient Hydrogen Evolution. ACS Appl. Mater. Interfaces 2021, 13, 56035-56044.

13 Gao, T.; Tang, X.; Li, X.; Wu, S.; Yu, S.; Li, P.; Xiao, D.; Jin, Z. Understanding the Atomic and Defective Interface Effect on Ruthenium Clusters for the Hydrogen Evolution Reaction. ACS Catal. 2023, 13, 49−59.
14 Wang, H.; Yang, P.; Liu, D.; Yu, M.; Zhou, B.; Zhang, Y.; Xiao, Z.; Xiao, W.; Wu, Z.; Wang, L. Ultrasmall RuM (Mo, W, Cr) Decorated on Nitrogen-doped Carbon Nanosheet with Strong Metal-support Interactions for Electrocatalytic Hydrogen Generation in Wide pH Range. J. Colloid Interface Sci. 2023, 651, 686−695.
15 Luo, H.; Zhang, X.; Zhu, H.; Zhang, K.; Yang, F.; Xu, K.; Yu, S.; Guo, D. Tailoring d-band center over electron traversing effect of NiM@C-CoP (M=Zn, Mo, Ni, Co) for high-performance electrocatalysis hydrogen evolution. J. Mater. Sci. Technol. 2023, 166, 164−172.
16 Li, Q.; Gao, Y.; Liu, M.; Xiao, W.; Xu, G.; Li, Z.; Liu, F.; Wang, L.; Wu, Z. Ultrafast synthesis of halogen-doped Ru-based electrocatalysts with electronic regulation for hydrogen generation in acidic and alkaline media. J. Colloid Interface Sci. 2023, 646, 391−398.
17 Zhang, J.; Zhang, Z.; Zhang, H.; Mei, Y.; Zhang, F.; Hou, P.; Liu, C.; Cheng, H.; Li, J. Prussian-Blue-Analogue-Derived Ultrathin Co2P-Fe2P Nanosheets for Universal-pH Overall Water Splitting. Nano Lett. 2023, 23, 8331−8338.
18 Shen, S.; Wang, Z.; Lin, Z.; Song, K.; Zhang, Q.; Meng, F.; Gu, L.; Zhong, W. Crystalline-Amorphous Interfaces Coupling of CoSe2/CoP with Optimized d-Band Center and Boosted Electrocatalytic Hydrogen Evolution. Adv. Mater. 2022, 34, 2110631.